ISSN 0915-633X

NATIONAL INSTITUTE FOR FUSION SCIENCE

Statistical Properties of the Neoclassical Radial Diffusion in a Tokamak Equilibrium

A. Maluckov, N. Nakajima, M. Okamoto, S. Murakami and R. Kanno

(Received - Mar. 1, 2001)

NIFS-689 Apr. 2001

RESEARCH REPORT
NIFS Series

TOKI, JAPAN

Statistical properties of the neoclassical radial diffusion in a tokamak equilibrium

A Maluckov† , N Nakajima‡ , M Okamoto‡ , S Murakami ‡ and R Kanno‡

† Department of Fusion Science, The Graduate University for Advanced Studies, Toki, Gifu, 509-5292, Japan

‡ National Institute for Fusion Science, Toki, Gifu, 509-5292, Japan

E-mail: sandra@nifs.ac.jp

Abstract. The statistical properties of the neoclassical radial diffusion are confirmed through direct comparision with a Wiener process by the numerical evaluations of the cumulant, diffusion and autocorrelation coefficients. Within the neoclassical framework the origin of stochasticity exists only in velocity space. It is characterized by the stationary, subdiffusive, uniform and Markov process. Through the drift motion of particle guiding centers, the stochasticity in velocity space leads to that in configuration space, i.e., the radial diffusion. It is shown that such a radial diffusion develops as an approximately Wiener process, i.e. the statistically non-stationary, normal diffusive, Gaussian, and Markov process in the asymptotic time region.

Keywords: neoclassical diffusion, statistics, autocorrelation, Cumulant, Gaussian process, Markovian process, Winner process

1. Introduction

The neoclassical transport theory [1, 2] is the basis of the plasma transport in a topologically torus geometry with magnetic field consisting of regular nested flux surfaces. In this framework, the deterministic drift motion of particle guiding centers inherent in such a geometry and the stochasticity due to the Coulomb collision in velocity space completely determine the neoclassical radial diffusion process in configuration space. Properties of the neoclassical radial diffusion are categorized quantitatively according to the relative magnitude between the characteristic frequency of the stochasticity (Coulomb collision frequency) ν and those of the drift motion. In axisymmetric tokamaks, the deterministic drift motion of guiding centers has two types of characteristic frequency; one is a bounce frequency ν_b, and the other is a transit frequency ν_t. Thus, three asymptotic regimes exist: collisionless banana regime ($\nu \ll \nu_b$), intermediate plateau regime ($\nu_b \ll \nu \ll \nu_t$), and collisional Pfirsch–Schlüter regime ($\nu_t \ll \nu$). For each asymptotic regime, the diffusion coefficient is obtained by using a variational approach [1] or a moment approach [2].

The neoclassical transport in a torus geometry with a perturbed magnetic field has been investigated under various circumstances [3, 4, 5, 6]. In these cases, the perturbed magnetic field is treated as a statistical quantity, so there are two types of statistical quantities; one is the stochastic velocity due to the Coulomb collision, and the other is the stochastic magnetic field. The former influences the neoclassical radial diffusion from the velocity space, and the latter does from the configuration space. In order to clarify statistical properties of the radial diffusion in a magnetic field with a partially or fully developed stochastic component, we must carefully examine the effect of each type of stochastic quantity.

In this paper, as a first step, statistical properties of the standard neoclassical transport of electrons in an axisymmetric tokamak are investigated. In this standard case, there is no magnetic field perturbation, so that there is not a direct stochastic source in configuration space, but an indirect stochastic source due to the Coulomb collision in velocity space. The Monte Carlo technique, consisting of the dynamical part (drift motion of guiding centers) and statistical part (Coulomb collision in velocity space), is used. We clarify the statistical properties from the viewpoint of the type of diffusive behaviour, Gaussianity, statistical stationarity, and Markovianity directly comparing the neoclassical radial diffusion with a Wiener process. For such a purpose, the cumulant (up to the 4th order) and autocorrelation coefficients of the radial displacement of guiding centers are observed.

The working model is briefly described in section 2. After statistical measures are defined in section 3.1, they are used to declare statistics of the Wiener and pitch angle scattering processes in sections 3.2 and 3.3, respectively. In section 3.4.1 the radial diffusion is clarified as a Wiener like process in the long time limit. The ballistic short time response of the system is mentioned in section 3.4.2. Finally, conclusion is written in section 4.

2. Model

2.1. Theoretical development

The neoclassical transport is evaluated by the solution of the gyro-phase averaged Boltzman equation. The distribution function of the gyro-phase averaged Boltzman equation is the function of time t, position $\boldsymbol{r}$, energy E, and magnetic moment μ. In this study, for simplicity, only pitch angle scattering of the linearized Coulomb collision operator is retained as the collision term. Hence, the energy E of each guiding center particle is conserved and only the magnetic moment μ is changed by the Coulomb collision.

In such a situation, the gyro-phase averaged Boltzman equation is expressed by

$$\frac{\partial f}{\partial t} + \boldsymbol{v} \cdot \nabla f = C(f) \tag{1}$$

where $f = f(t, \boldsymbol{r}, \mu)$ and $C(f)$ is the linearized pitch angle scattering due to the Coulomb collision. The particle drift velocity $\boldsymbol{v}$ in the magnetic field with nested regular flux surfaces is given by [7]

$$\boldsymbol{v} = v_{\parallel} \frac{\boldsymbol{B} + \nabla \times (\rho_{\parallel} \boldsymbol{B})}{B + \hat{n} \cdot \nabla \times (\rho_{\parallel} \boldsymbol{B})} \tag{2}$$

where $v_{\parallel}$ is the parallel velocity ($v_{\parallel} = \boldsymbol{v} \cdot \hat{n}$), $\rho_{\parallel} \equiv v_{\parallel}/\Omega$ with the gyrofrequency Ω, and $\hat{n} \equiv \boldsymbol{B}/B$.

Instead of solving equation (1) directly, the Monte Carlo technique is used [8]. Equations for each guiding center particle equivalent to equation (1) consist of two parts; the dynamical part (orbit part) and the stochastic part (Coulomb collision part). Since the characteristic equations of equation (1) without the collision term are obtained from

$$\dot{\xi} \equiv \frac{\mathrm{d}\xi}{\mathrm{d}t} = \boldsymbol{v} \cdot \nabla \xi \tag{3}$$

equations of the guiding center in the Boozer coordinates (ψ, θ, ζ) (ψ is the label of a flux surface defined as the toroidal flux/2π, θ and ζ are poloidal and toroidal angles, respectively) become

$$\begin{aligned}
\dot{\psi} &= -\frac{\delta}{\gamma}\left(J\frac{\partial B}{\partial \theta} - I\frac{\partial B}{\partial \zeta}\right) \\
\dot{\theta} &= \frac{\delta}{\gamma} J\frac{\partial B}{\partial \psi} + \frac{e^2 B^2}{\gamma m}\rho_{\parallel}\left(\iota - \rho_{\parallel}\frac{dJ}{d\psi}\right) \\
\dot{\zeta} &= -\frac{\delta}{\gamma} I\frac{\partial B}{\partial \psi} + \frac{e^2 B^2}{\gamma m}\rho_{\parallel}\left(1 + \rho_{\parallel}\frac{dI}{d\psi}\right) \\
\dot{\rho}_{\parallel} &= -\frac{\delta}{\gamma}\left(\left(\iota - \rho_{\parallel}\frac{dJ}{d\psi}\right)\frac{\partial B}{\partial \theta} + \left(1 + \rho_{\parallel}\frac{dI}{d\psi}\right)\frac{\partial B}{\partial \zeta}\right)
\end{aligned} \tag{4}$$

where the energy conservation is used, and

$$\gamma = e\left(J\left(1 + \rho_{\parallel}\frac{dI}{d\psi}\right) + I\left(\iota - \rho_{\parallel}\frac{dJ}{d\psi}\right)\right)$$

$$\delta = \mu + \frac{e^2 B}{m}\rho_{\|}^2$$

with the rotational transform ι, the magnetic moment μ, the poloidal (toroidal) current outside (inside) the flux surface $2\pi J(\psi)$ $(2\pi I(\psi))$. The radial coordinate r is related to ψ as $r/a = \sqrt{\psi(r)/\psi(a)}$ where a is the minor radius.

The pitch angle scattering process in equation (1) is expressed as

$$\frac{\partial f}{\partial t} = C(f) = \frac{\nu}{2}\frac{\partial}{\partial \lambda}\left((1-\lambda^2)\frac{\partial f}{\partial \lambda}\right) \tag{5}$$

where the pitch angle $\lambda = v_{\|}/v$ is used instead of the magnetic moment μ, and ν is the deflection collision frequency. Knowing the solution of equation (5) with the initial condition $f(\lambda, t=0) = \delta(\lambda - \lambda_0)$, a Langevin equation giving the same mean value of $\langle\lambda\rangle$ and standard deviation σ is constructed [8]

$$\frac{d\lambda}{dt} + \nu\lambda = F(t) \tag{6}$$

defining the stochastic source $F(t)$ with $\langle F(t)\rangle = 0$ and the autocorrelation giving σ. From the solution of equation (6), for a discrete time step Δt satisfying $\Delta t\nu \ll 1$, λ is changed as

$$\lambda(t_n) = \lambda(t_{n-1})(1-\nu\Delta t) \pm \sqrt{(1-\lambda^2(t_{n-1}))\nu\Delta t}, \tag{7}$$

for one step from $t_{n-1} = (n-1)\Delta t$ to $t_n = n\Delta t$. The symbol $\pm$ indicates that the sign is to be chosen randomly, but with equal probability for plus and minus.

Since a given magnetic field and the linearized Coulomb collision operator are used, each guiding center particle is completely independent of others. The pitch angle scattering due to the Coulomb collision in velocity space introduces stochastic properties in the system or in configuration space, so that the particle ensemble allows statistical treatment.

2.2. Numerical model

The electron guiding center equations given by equation (4) are solved using 8th order Runge–Kutta method. The pitch angle scattering due to the Coulomb collision is added following reference [4] at every particle orbit time step. In order to eliminate numerical errors and obtain good statistics, the number of guiding center particles N is chosen to be 10000. The energy of all electrons is fixed as $E = 3\text{keV}$ and the relative error of the energy conservation is tolerated up to $10^{-4}\%$ during the calculations.

As a MHD equilibrium, an axisymmetric FCT tokamak with regular nested flux surfaces is adopted. The boundary is circular, $B = 3\text{T}$, and the major and minor radii are $R = 3\text{m}$ and $a = 1\text{m}$, respectively. The profile of the rotational transform is specified as $\iota = 0.9 - 0.5875(r/a)^2$, and $\beta =$ (kinetic pressure/magnetic pressure) $= 0$. All particles are initially started from the same flux surface with $\iota = 2/3$ at $r/a = 0.63$, with uniformly distributed poloidal and toroidal angles in the Boozer coordinates and with randomly chosen pitch angles.

Statistical properties of the neoclassical radial diffusion

The system has two types of characteristic frequencies associated with the particle dynamics: the transit frequency of passing particles ν_t and the bounce frequency of trapped particles ν_b. The characteristic times are $\tau_t(=\nu_t^{-1})$ for passing and $\tau_b(=\nu_b^{-1})$ for trapped particles, respectively. Both frequencies and characteristic times at the initial flux surface are [9]

$$\begin{aligned} \nu_t &= \frac{\iota v}{\pi R} &&= 2.21\times 10^6\ \mathrm{s}^{-1} \ : \ \tau_t=\nu_t^{-1} &&= 4.35\times 10^{-7}\ \mathrm{s} \\ \nu_b &= \left(\frac{r}{R}\right)^{3/2}\nu_t &&= 2.30\times 10^5\ \mathrm{s}^{-1} \ : \ \tau_b=\nu_b^{-1} &&= 4.52\times 10^{-6}\ \mathrm{s} \end{aligned} \tag{8}$$

where $v=\sqrt{2E/m}$. According to the relative magnitude among above characterictic frequencies (times) associated with particle dynamics and the deflection collision frequency ν (collision time, $\tau_c=\nu^{-1}$) due to the Coulomb collision associated with stochasticity, there are three types of collisionality regime:

$$\begin{aligned} &\nu \ll \nu_b \ll \nu_t \quad \text{or} \quad \tau_c \gg \tau_b \gg \tau_t \ : \ \text{banana regime} \\ &\nu_b \ll \nu \ll \nu_t \quad \text{or} \quad \tau_b \gg \tau_c \gg \tau_t \ : \ \text{plateau regime} \\ &\nu_b \ll \nu_t \ll \nu \quad \text{or} \quad \tau_b \gg \tau_t \gg \tau_c \ : \ \text{Pfirsch- Schlüter regime.} \end{aligned} \tag{9}$$

In the simulation different collisional regimes are treated by choosing the parameter ν to be $10^4\mathrm{s}^{-1}$, $10^6\mathrm{s}^{-1}$ and $10^7\mathrm{s}^{-1}$, which corresponds to the banana, plateau and Pfirsch-Schlüter regime, respectively. In order to satisfy above mentioned energy conservation, the time step size Δt of the numerical calculation is adopted to be $\Delta t = 0.5\cdot 10^{-9}\mathrm{s}$.

3. Statistics of the neoclassical diffusion

3.1. Statistical measures

The statistical analysis of the radial diffusion is based on calculation of the cumulant, diffusion and autocorrelation coefficients. They are defined with respect to the radial particle displacement

$$\delta r(t) = r(t) - r(0)$$

From now, the symbol $\langle X\rangle$ denotes particle ensemble average

$$\langle X\rangle = \frac{1}{N}\sum_{i=1}^{N} X_i \tag{10}$$

where N is the number of particles in the observed particle ensemble.

The dimensionless n-th cumulant coefficient γ_n [10] is given by

$$\gamma_n(t) = \frac{C_n(t)}{C_2^{n/2}(t)} \tag{11}$$

where $C_n(t)$ is n-th cumulant. Up to the 4th order it is calculated as [11]

$$C_1(t) = \langle \delta r(t)\rangle, \tag{12}$$

$$C_n(t) = \langle (\delta r(t) - \langle \delta r(t)\rangle)^n\rangle, \qquad n=2,3 \tag{13}$$

$$C_4(t) = \langle(\delta r(t) - \langle\delta r(t)\rangle)^4\rangle - 3C_2^2(t). \tag{14}$$

The first cumulant is a measure of the advective effect or convective diffusion [11]. This advective effect is eliminated from the higher cumulants. The second cumulant is the dispersion around $\langle r(t)\rangle$, and a measure of the conductive diffusion, from which the time dependent diffusion coefficient is defined as

$$D(t) = \frac{C_2(t)}{2t} \tag{15}$$

The time dependence of C_2

$$C_2(t) \approx t^{\alpha}, \tag{16}$$

determines the nature of a stochastic process [12]. The process with $\alpha < 1, = 1, > 1$ is a subdiffusive, normal diffusive, or superdiffusive process, respectively. Corresponding diffusion coefficient is defined as

$$D(t) \approx t^{\alpha-1}. \tag{17}$$

It is proved [10] that the only physically acceptable random process with a finite number of nonvanishing cumulant coefficients is Gaussian with $\gamma_{n>2} = 0$. Therefore, the cumulant coefficients $\gamma_{n>2}$ generically carry information about non-Gaussianity [13] ‡. The degree of asymmetry around $\langle r(t)\rangle$ and relative peakenness or flatness of a particle distribution, with respect to Gaussian, are characterized by γ_3 (skewness), and γ_4 (kurtosis), respectively. A positive (negative) value of skewness signifies a distribution with an asymmetric tail extending out towards $r(t) > \langle r(t)\rangle$ ($r(t) < \langle r(t)\rangle$), and a positive (negative) value of kurtosis indicates more peaked (flated) distribution than the Gaussian one.

The autocorrelation coefficient [11, 14] is given by

$$A(t,t') = \frac{\langle(\delta r(t) - \langle\delta r(t)\rangle)(\delta r(t') - \langle\delta r(t')\rangle)\rangle}{\sqrt{\langle(\delta r(t) - \langle\delta r(t)\rangle)^2\rangle\langle(\delta r(t') - \langle\delta r(t')\rangle)^2\rangle}}. \tag{18}$$

If the autocorrelation coefficient $A(t,t')$ depends only on the time interval $\tau = t' - t$ the process is statistically stationary. On the other hand, when $A(t,t')$ is the function of both times t and t', the process is statistically non-stationary.

The Markovianity of a stochastic process means that the stochastic process is fully determined by the knowledge of probability density at any fixed time and transition probabilities from that state to the arbitrary ones. The deterministic process is of Markov type. If one process is Gaussian and Markovian then following equality is true [14]

$$A(t,t') = A(t,t'')A(t'',t') \text{ for } t \le t'' \le t' \text{ or } t \ge t'' \ge t', \tag{19}$$

and if equation (19) is true for a Gaussian process then it is Markovian.

‡ The non-Gaussianity is then attached to the existence of the correlation effects in the treated stochastic process

3.2. The Wiener process

In order to clarify the statistical measures mentioned above, those measures are applied to the well-known Wiener process [12, 15]. The Wiener process is fundamental to the study of diffusion processes. It is a Markov process described by the Langevin equation as the integral of the white noise, $F(t)$

$$\frac{\mathrm{d}x}{\mathrm{d}t} = F(t), \tag{20}$$

with

$$\langle F(t) \rangle = 0, \qquad \langle F(t)F(t') \rangle = \mathcal{D}\delta(t - t')$$

where $\mathcal{D}$ is constant and $x(t)$ is the particle position.

By using equations (12) and (13) for $\delta x(t) = x(t) - x_0$,

$$C_1(t) = 0, \qquad C_2(t) = \mathcal{D}t \tag{21}$$

where x_0 is the particle position at $t = 0$. The second cumulant is expressed as a linear function of time, so that the diffusion coefficient given by equation (15) is

$$D = \frac{\mathcal{D}}{2}$$

Hence, the Wiener process is normal diffusive.

The skewness and kurtosis are

$$\gamma_3 = 0, \qquad \gamma_4 = 0$$

The normal diffusivity and vanishing skewness and kurtosis suggest that the Wiener process is Gaussian. Indeed, since the values of variable $x(t)$ are independent random events (from the white noise stochastic origin indicated by equation (20)), the probability distribution and conditional probability are Gaussians as the center limit theorem shows [13, 15]. Hence, the conditional (transition) probability is given by

$$f(x, t|x_0, 0) = \frac{1}{\sqrt{(2\pi\mathcal{D}t)}} \exp\left(\frac{(x - x_0)^2}{2\mathcal{D}t}\right),$$

which is the solution of the Fokker-Plank equation

$$\frac{\partial}{\partial t} f(x, t|x_0, 0) = \frac{\mathcal{D}}{2} \frac{\partial^2}{\partial x^2} f(x, t|x_0, 0)$$

with the initial condition $f(x, 0|x_0, 0) = \delta(x - x_0)$.

On the other hand, by using

$$\langle \delta x(t) \delta x(t') \rangle = \mathcal{D}\min(t, t'),$$

the autocorrelation coefficient (equation (18)) is

$$A(t, t') = \sqrt{\frac{t}{t'}}, \qquad \text{for} \qquad t \leq t', \tag{22}$$

which indicates that the Wiener process is statistically non-stationary. The autocorrelation coefficients satisfy equation (19). It is consistent with the Gaussianity and Markovianity of the Wiener process.

Therefore, from the statistical point of view, the Wiener process is a Markov, normal diffusive, Gaussian and non-stationary process.

3.3. Statistical properties of the pitch angle scattering

The statistical characteristics of the pitch angle scattering (velocity space stochasticity origin in the neoclassical radial diffusion) can be determined analytically by a conditional probability $f(\lambda, t|\lambda_0, 0)$ with the initial condition [15]

$$f(\lambda, 0|\lambda_0, 0) = \delta(\lambda - \lambda_0) \tag{23}$$

satysfying the Fokker-Plank equation (5). Therefore, the pitch angle scattering is a Markov process, i.e. the knowledge of the general solution of equation (5) (the pitch angle conditional probability)

$$f(\lambda, t|\lambda_0, 0) = \sum_{n=0}^{\infty} \frac{2n+1}{2} P_n(\lambda_0) P_n(\lambda) \exp\left(\frac{-n(n+1)\nu t}{2}\right) \tag{24}$$

where $P_n(\lambda)$ is the Legendre polynomial [16], fully determines the pitch-angle scattering.

Using the orthonormallity relations of the Legendre polynomials

$$\int_{-1}^{1} d\lambda P_m(\lambda) P_n(\lambda) = \frac{2}{2n+1} \delta_{n,m}, \tag{25}$$

average with respect to $f(\lambda, t|\lambda_0, 0)$

$$\langle X(\lambda) \rangle = \int_{-1}^{1} d\lambda X(\lambda) f(\lambda, t|\lambda_0, 0), \tag{26}$$

and calculating the statistical measures with respect to $\lambda(t)$, the values of the first and second cumulants (equations (12) and (13)) are

$$C_1(t) = \lambda_0 \mathrm{e}^{-\nu t} \tag{27}$$

and

$$C_2(t) = \lambda_0^2 (\mathrm{e}^{-3\nu t} - \mathrm{e}^{-2\nu t}) + \frac{1}{3}(1 - \mathrm{e}^{-3\nu t}) \tag{28}$$

The straightforward calculations (equations (11)-(14)) give the values of cumulants in the limit $\nu t \gg 1$

$$C_1 = 0, \qquad C_2 = \frac{1}{3}, \qquad \gamma_{2n+1} = 0, \qquad \gamma_4 = -\frac{6}{5} \tag{29}$$

and

$$\gamma_{2n} \neq 0, \qquad n = 1, 2, .. \tag{30}$$

The finite constant value of C_2 declares the pitch angle scattering as a subdiffusive process (in the asymptotic region $\nu t \gg 1$). On the other hand, $\gamma_{2n+1} = 0$ and finite γ_{2n} are characteristics of the symmetric broad distribution. In the asymptotic time limit ($\nu t \gg 1$), it becomes the uniform distribution $f(\lambda, t) \to 1/2$, namely it is a uniform process.

The calculations of two time autocorrelation functions give

$$\langle (\lambda(t) - \langle \lambda(t) \rangle)(\lambda(t') - \langle \lambda(t') \rangle) \rangle = (\lambda_0^2 - \frac{1}{3}) \mathrm{e}^{-\nu(t'+2t)} + \frac{1}{3} \mathrm{e}^{-\nu(t'-t)} - \lambda_0^2 \mathrm{e}^{-\nu(t+t')} \tag{31}$$

Hence, the autocorrelation coefficient according to equation (18) is

$$A(t,t') = \mathrm{e}^{-\nu(t'-t)}, \qquad t' \geq t \tag{32}$$

when $\nu t \gg 1$. Since $A(t,t')$ is the function only of $t'-t$, the pitch angle scattering is a statistically stationary process.

The analitically predicted statistical properties of the pitch angle scattering are checked by the same numerical procedure as that established for the treatment of the radial diffusion. The numerical calculations are started with ensemble of $N = 10000$ independent particles, whose pitch angle distribution is obtained by uniform random number generator. For a fixed parameter ν, at each time step ($\Delta t = 0.5 \cdot 10^{-8}$s) the pitch angle of each particle is changed by the Monte Carlo procedure (equation (7)). The statistical procedure in section 3.1 gives the values of cumulants which are scattered around the analytical ones (equation (29))

$$C_1(t) = (0.0 \pm 10^{-6}), \quad C_2(t) = (\frac{1}{3} \pm 0.002), \quad \gamma_3(t) = (0.0 \pm 0.01) \tag{33}$$

and

$$\gamma_4(t) = (-\frac{6}{5} \pm 0.01) \tag{34}$$

where the second number in brackets shows maximum discrepance from the analytical estimations.

Additionally, the calculations of the autocorrelation coefficients give

$$A(t,t') \approx \mathrm{e}^{-(t'-t)/t_{corr}}, \qquad t' \geq t \tag{35}$$

where the correlation time is $t_{corr} = \nu^{-1}$.

Therefore, the numerically obtained statistical properties of the pitch angle scattering are consistent with the analytical ones.

3.4. Statistical properties of the radial diffusion

Since the neoclassical transport is determined by the synergetic effect between particle drift motion [deterministic part] and Coulomb collision (in our case, pitch angle scattering) [stochastic part], it is expected that the temporal behaviour of statistical properties changes beyond the slowest time scale among that of the trapped and passing particle orbits, and stochastic pitch-angle scattering. Thus, a system characteristic time is according to section 2.2.

$$\tau_s \sim \begin{cases} \tau_c & \text{for banana regime} \\ \tau_b & \text{for plateau regime} \\ \tau_b & \text{for Pfirsch-Schlüter regime} \end{cases} \tag{36}$$

It is considered that the system is in transient phase for $t \leq \tau_s$, and the time region $t \gg \tau_s$ is specified as the asymptotic time region.

Statistical properties of the neoclassical radial diffusion

In the standard neoclassical theory, the radial diffusion is treated as the normal diffusive process. For each collisionality regime, the analytical diffusion coefficient is given by [9]

$$\begin{aligned} D_{PS} &= D_p \frac{\nu}{\nu_t} && : \text{for} \quad \nu_t \ll \nu \\ D_p &= 0.64 \times \frac{\rho^2 v}{\pi t R} = 1.24 \times 10^{-2}\ \mathrm{m}^2/\mathrm{s} && : \text{for} \quad \nu_b \ll \nu \ll \nu_t \\ D_b &= D_p \frac{\nu}{\nu_b} && : \text{for} \quad \nu \ll \nu_b \end{aligned} \tag{37}$$

where $\rho = mv/(eB)$ is the Larmor radius. In figure 1 the analytical diffusion coefficient is plotted as the function of parameter ν (solid line).

In the followings, the stochastic properties of the radial diffusion are numerically analyzed for each collisionality regime. The corresponding collision frequencies are shown in figure 1: $\nu = 10^4, 10^6$, and $10^7\ \mathrm{s}^{-1}$ for banana, plateau, and Pfirsch-Schlüter collisionality regime, respectively. The ratios among various characteristic times are given, using equation (8), by

$$\begin{aligned} \tau_s = \tau_c : \tau_b : \tau_t &= 1 : 0.0425 : 0.00435 && \text{banana regime} \\ \tau_s = \tau_b : \tau_c : \tau_t &= 1 : 0.218 : 0.095 && \text{plateau regime} \\ \tau_s = \tau_b : \tau_t : \tau_c &= 1 : 0.095 : 0.0218 && \text{Pfirsch-Schlüter regime.} \end{aligned} \tag{38}$$

The normal diffusivity of the radial diffusion is proved by the numerical calculations of the second cumulant (equation (13)), and the diffusion coefficient (equation (15)). In figure 2, $C_2(t)$ is plotted with respect to t. The normal diffusive response of system

$$C_2(t) \approx t \tag{39}$$

in all collisional regimes is followed by the saturation of the diffusion coefficient (figure 3)

$$D \approx const., \qquad t > \tau_s \tag{40}$$

Estimations give $D = (0.0004, 0.013, 0.056)\mathrm{m}^2\mathrm{s}^{-1}$ for the banana, plateau, and Pfirsch-Shlüter regimes, respectively. These are consistent with the analytical neoclassical results indicated in figure 1 (dots on the curve).

The calculations of $C_1(t)$ (equation (12)) show that the convective effect is irrelevant ($|C_1(t)| = |\langle \delta r(t) \rangle| \approx 10^{-5} a \approx \rho_{||}$) in all collisional regimes.

The time behaviours of skewness (γ_3), and kurtosis (γ_4) are investigated in order to see relation with Gaussianity. The values of skewness tend to $|\gamma_3| \approx 0.02$ ($t \gg \tau_s$) in figure 4, which indicates a highly symmetric particle radial distribution with respect to $\langle r(t) \rangle \approx r(t=0)$ in all collisional regimes. The normalized drift widths of passing Δ_p/a and trapped Δ_t/a particles (electrons) at the initial magnetic surface are given by

$$\frac{\Delta_p}{a} = \frac{\rho_{||}}{\iota a \sqrt{\varepsilon}} = 9.2 \cdot 10^{-5}$$

and

$$\frac{\Delta_t}{a} = \frac{\rho_{||}}{\iota a} = 2.0 \cdot 10^{-4}$$

where $\varepsilon = r(t=0)/R = 0.21$. These values are so small that electrons could not feel asymmetry of the system, even if their orbits are asymmetric around their initial magnetic surfaces.

Figure 5 shows tendency of kurtosis to reduce to $|\gamma_4| \approx 0$ in asymptotic time region, $t \gg \tau_s$, or more strictly, $t > 20\tau_s$ in the collisionless, and $t > 5\tau_s$ in the collisional regimes. Thus, the obtained time behaviour of γ_4 illustrates the particularity of the collisionless regime, or generally, of the time regions where the stochastic scatterings weakly affect the particle orbit motion (transient time regions in all collisional regimes). The particle orbit effects strongly affect the radial diffusion in the collisionless regime by slowing down relaxation of kurtosis to $\gamma_4(t) \approx 0$. The transient positive value of kurtosis in the collisionless banana regime (solid line in figure 5) indicates a more peaked (at $r(t) = \langle r(t) \rangle$) distribution function than Gaussian (rare stochastic scatterings yet can not produce the significant radial displacement of ensemble constituent majority from the regular drift surfaces). On the other hand, the negative transient values of kurtosis observed in the collisional Pfirsch-Schlüter regime (dotted curve in figure 5), correspond to a more flated distribution than Gaussian (particles wander across areas in the neighbourhood of the earlier regular drift surfaces).

Note that the vanishing $\gamma_{3,4}$ in the asymptotic time limit $t \gg \tau_s$, only suggests the Gaussianity of the radial diffusion [10,13] in the long time limit.

To investigate the statistical stationarity in figures 6(a), 6(b), and 6(c) the autocorrelation coefficients $A(t,t')$ given by equation (18) are plotted with respect to $\tau = t'-t$, and starting time, t, chosen to be $(2\times10^{-3}, 1.6, 3.2, ..., 12.8)\tau_s$, $(4\times10^{-3}, 1, ..., 8)\tau_s$, and $(2\times10^{-2}, 1, ..., 8)\tau_s$, for the radial diffusion in the banana, plateau, and Pfirsch-Schlüter regimes (solid lines), respectively. As t increases the form of $A(t,t')$ curves changes (figures 6(a), 6(b), and 6(c)). This inidicates the statistical non-stationarity of the radial diffusion. Additionally, the fine structures are observed in the power-law like autocorrelation curves. In the collisionless (banana) regime (figure 6(a)) they are the result of the characteristic trapped and passing particle periodic motions, which are weakly affected by rare stochastic events ($\tau_s = \tau_c \gg \tau_b > \tau_t$). As the stochastic small particle deflections from the regular drift orbits become more frequent ($\tau_s = \tau_b > \tau_c, \tau_t$, the collisional regimes), the autocorrelation curves become more smooth (figures 6(b), and 6(c)).

From the statistical analysis up to now, the radial diffusion has been regarded as a normal diffusive and statistically non-stationary process, whose the first cumulant $C_1(t)$, the third and the fourth cumulant coefficients $\gamma_{3,4}$ almost vanish in the asymptotic time limit. These statistical properties are a part of those of the Wiener process mentioned in section 3.2. Therefore, it is meaningful to directly compare $A(t,t')$ of the neoclassical radial diffusion with the corresponding Wiener ones in the asymptotic time limit $t \gg \tau_s$.

3.4.1. Comparision with a Wiener process In figures 6(a), 6(b), and 6(c) the autocorrelation coefficients $A(t,t')$ for the radial diffusion in the banana, plateau and Pfirsch-Schlüter regime (solid curves) are compared with the Wiener ones (dotted

curves) which are given by equation (22). The time behaviour of the autocorrelation coefficients is well approximated by the Wiener process with the increase in t in all collisional regimes. Namely, in the asymptotic time limit, the neoclassical radial diffusion tend to become a Wiener like process. This is more clear with the increase in $\tau = t' - t$. According to the absence of any time correlation effect in the Wiener process the deviations of $A(t, t')$ in the asymptotic time limit from the Wiener ones may be related to the existence of the short time correlations. Also, figures (6(a),6(b), and 6(c)) show that tendency of the radial diffusion $A(t, t')$ curves to fit to the Wiener ones is slower in the collisionless than in the collisional regimes. It appears since the particle orbit motion is less affected by collisions in the banana regime with $\tau_c \gg \tau_b > \tau_t$ than in the plateau and Pfirsch-Schlüter regimes with the characteristic time ordering $\tau_b > \tau_c > \tau_t$ and $\tau_b > \tau_t > \tau_c$, respectively.

In order to confirm above observations from figure 6, the coefficient y, associated with equation (19), is calculated

$$y = \frac{A(t, t'')A(t'', t')}{A(t, t')} - 1, \quad t < t'' < t' \tag{41}$$

For a Wiener process $y = 0$. The numerical values of $A(t, t')$ are collected on time scale whose unit step and starting time are $\Delta t = 0.1\tau_s$ and $t = (0.5, 1, 2, 3, 5)\tau_s$, respectively. Therefore, $t'' = t + m\Delta t$ and $t' = t'' + n\Delta t$, where $m, n = 1, 2....$ In table 1 the maximum values of $|y|$ are shown for the banana ($\nu = 10^4 \mathrm{s}^{-1}$), plateau ($\nu = 10^6 \mathrm{s}^{-1}$), and Pfirsch-Schlüter ($\nu = 10^7 \mathrm{s}^{-1}$) regime, respectively. The radial diffusion process in the plateau regime is the best approximated by a Wiener process ($\tau_s = \tau_b > \tau_c > \tau_t$).

Generally, the values of $|y|_{max}(t)$ decrease as the starting time t increases and average values of deviations, $\langle y \rangle$, given in table 2 tend to the Wiener one $\langle y \rangle = 0$ in all collisional regimes.

It supports above mentioned tendency of the radial diffusion $A(t, t')$ curves to fit better to the Wiener ones in the asymptotic time limit $t \gg \tau_s$.

Therefore, the neoclassical radial diffusion developes as a normal diffusive, statistically non-stationary, Markov and Gaussian process in the long time limit, i.e. it is a Wiener like process.

3.4.2. The short time ballistic phase The short time , $t \approx \tau_t \ll \tau_s$, ballistic phase characterized by

$$C_2(t) \approx t^2 \qquad \text{and} \qquad D(t) \approx t \tag{42}$$

is detected in all collisional regimes (figures 7 and 8). During it particles "freely" follow corresponding regular drift orbits. The collisional effects, which introduce stochasticity in the system, can not enough affect the particle motions as long as τ_c is higher or the same order as τ_t, and the ballistic phase is observed. In the banana ($\tau_c = 10^{-4}\mathrm{s}$), plateau ($\tau_c = 10^{-6}\mathrm{s}$), and Pfirsch-Schlüter ($\tau_c = 10^{-7}\mathrm{s}$) regimes, $\tau_c \gg \tau_t$, $\tau_c > \tau_t$, and $\tau_c \approx \tau_t$, respectively. Hence, the short time ($t \approx \tau_t$) ballistic behaviour is found in all collisional regimes.

4. Conclusion

The radial diffusion in the destroyed magnetic field topology is a realization of stochasticity in both the velocity space (collisional effect) and configuration space (magnetic field perturbation). Hence, in order to examine the statistical properties of the radial diffusion, the influence of two types of stochasticity must be investigated carefully. As the first step the statistics of the radial diffusion in a regular nested magnetic field configuration is studied. There, the stochasticity origin exists only in velocity space. It generates stochasticity in configuration space, i.e. the radial diffusion through the drift particle motion.

The system of the test electron particle ensemble and stationary plasma background (whose characteristics are denoted by free parameter ν), which influences the behaviour of the test ensemble throught the pitch angle scattering (stochasticity origin from velocity space), is established by the Monte Carlo guiding center particle model.

Statistically, the pitch angle scattering is developed as a Markov, stationary, subdiffusive and uniform random process in the long time limit. Corresponding correlation time is the collisional time, τ_c. Without collisions guiding centers draw periodic trapped and passing motions in the configuration space whose characteristic times are the bounce time, τ_b, and transit time, τ_t, respectively. The stochasticity of pitch angle scattering interferes with those deterministic trapped and passing particle motions. Since the system relaxes beyond the slowest characteristic time scale, it is shown that according to the parameter $\tau_c = 1/\nu$, the system relaxation time τ_s, is τ_c and τ_b, for the collisionless (banana) and collisional (plateau and Pfirsch-Schlüter) regimes, respectively. It is numerically found that in the asymptotic time region ($t \gg \tau_s$) the radial diffusion in a regular magnetic field topology develops approximately as a Wiener process. Thus, the neoclassical radial diffusion is recognized as a normal diffusive, statistically non-stationary, Markov and Gaussian process. When the stochastic pitch angle scattering becomes rare, the relaxation to the Wiener process is only slowed down. This affects the particle radial distribution function through the transient non-Gaussianity and short time correlation effects, as is clearly shown by calculation of the cumulant and autocorrelation coefficients in the collisionless regime ($\tau_s = \tau_c \gg \tau_b > \tau_t$).

Finally, the short time ($t \approx \tau_t \ll \tau_s$) ballistic response is found in all collisionality regimes. It is result from a chosen τ_c which is larger than (banana) or the same order as τ_t (collisional cases), so that the collisional effect has not enough affected the deterministic particle orbit motion during $t \approx \tau_t$.

The next step will be to see how the coexistence of velocity and configuration space stochasticity origins govern the radial diffusion from the view point of statistical theory.

References

[1] Hinton F L and Hazeltine R D 1976 *Rev. Mod. Physics* **48** 309
[2] Hirshman S P and Sigmar V D 1981 *Nuclear Fusion* **21** 1079
[3] Rosenbluth M N, Sagdeev R Z, Taylor J B and Zaslavski G M 1966 *Nuclear Fusion* **6** 297

[4] Boozer A H and White R B 1982 *Phys. Rev. Lett.* **49** 786
[5] Wobig H and Fowler R H 1988 *Plasma Physics and Controlled Fusion* **30** 721
[6] Kovrizhnykh L M 1998 *Plasma Physics Reports* **24** 533
[7] Littlejohn R G 1983 *Journal of Plasma Physics* **29** 111
[8] Boozer A H and Kuo-Petravic G 1981 *Phys. Fluids* **24** 851
[9] Lotz W and Nührenberg J 1988 *Phys. Fluids* **31** 2984
[10] Dubkov A A and Malakhov A N 1977 *Radiophys. Quantum Electron.* **19** 833
[11] Van-Kampen N G 1981 *Stochastic Processes in Physics and Chemistry* (North-Holland)
[12] Balescu R 1997 *Matter out of Equilibrium* (Imperial Collage Press)
[13] Bouchand J-P and Georges A 1990 *Physics Reports* **195** No.4& 5 127-293
[14] Feller W 1971 *An Introduction of Probability Theory and Its Applications I,II* (John Wiley & Sons)
[15] Gardiner C W 1983 *Hanbook of Stochastic Methods for Physics, Chemistry and the Natural Sciences* (Springler-Verlag)
[16] Abramowitz M and Stegun A I 1972 *Handbook of Mathematical Functions* (Dover Publications, Inc. , New York) p. 772

Tables and table captions

Table 1. The maximum deviation of the autocorrelation coefficients, $|y|$, from the Wiener value $y = 0$ in the banana, plateau and Pfirsch-Schlüter regimes, with respect to the different starting times t/τ_s.

t/τ_s	$\nu = 10^4 s^{-1}$	$\nu = 10^6 s^{-1}$	$\nu = 10^7 s^{-1}$
0.5	0.2014	0.1009	0.0772
1	0.1753	0.0548	0.0744
2	0.1157	0.0383	0.0729
3	0.0970	0.0426	0.0438
5	0.0553	0.0181	0.0251

Table 2. The average value of the deviation y from the Wiener one $\langle y \rangle = 0$ in the banana, plateau and Pfirsch-Schlüter regime with respect to the starting time t/τ_s.

t/τ_s	$\nu = 10^4 s^{-1}$	$\nu = 10^6 s^{-1}$	$\nu = 10^7 s^{-1}$
0.5	0.0407	0.0050	0.0190
1	0.0567	0.0137	0.0274
2	0.0525	0.0061	0.0275
3	0.0416	0.0122	0.0162
5	0.0283	0.0001	0.0115

Figure captions

Figure 1. The comparision of the numerically and the analytically calculated [9] neoclassical diffusion coefficients (solid and dotted curve, respectively) for starting particles position $r/a = 0.63$ is shown. The numerical curve is obtained for ensemble of 10000 electrons, and only the pitch angle scattering is included. The values ν_b and ν_p correspond to the bounce frequency and transit frequency, respectively. The axes are plotted in log-log proportion.

Figure 2. The 2nd cumulant time behaviour for the collisionless ($\nu = 10^4 s^{-1}$), intermediate ($\nu = 10^6 s^{-1}$) and collisional regimes ($\nu = 10^7 s^{-1}$) is plotted by the solid, dashed and dotted curve, respectively. Time is normalized with respect to the system characteristic time τ_s.

Figure 3. The diffusion coefficients saturate to $D = 0.0004, 0.013$, and $0.056 m^2 s^{-1}$ for observed collisional cases $\nu = 10^4, 10^6$, and $10^7 s^{-1}$, as is indicated by solid, dashed and dotted curves, respectively.

Figure 4. The asymmetry of the particle distribution function is measured by the skewness, γ_3. In the banana (solid curve), plateau (dashed) and Pfirsch-Schlüter (dotted curve) regimes, deviations of γ_3 from the normal Gaussian distribution are small.

Figure 5. Kurtosis, γ_4, is the measure of the narrowness of the particle distribution function. The positive value of kurtosis in the banana regime (solid curve) indicate more peaked distribution function than Gaussian. On the other hand, the transient negative values of γ_4 in the Pfirsch-Schlüter regime (dotted curve) show more flated distribution than the Gaussian one. Kurtosis goes to zero in the asymptotic time limit.

Figure 6. The autocorrelation coefficients $A(t, t')$ vs $\tau = t' - t$ for the banana (6(a)), plateau (6(b)) and Pfirsch-Schlüter (6(c)) regimes. The solid curves are obtained by the numerical Monte Carlo procedure. The dotted ones which correspond to the Wiener process are calculated from equation (22). Starting time t is:

$$t = (2 \times 10^{-3}, 1.6, 3.2, ..., 12.8)\tau_s, \text{banana regime}$$
$$t = (4 \times 10^{-2}, 1, 2, ..., 8)\tau_s, \quad \text{plateau regime}$$
$$t = (2 \times 10^{-2}, 1, 2, .., 8)\tau_s, \quad \text{Pfirsch-Schlüter regime.}$$

Figure 7. The short time ballistic phase of the second cumulant for the banana (solid curve), plateau (dashed curve) and Pfirsch-Schlüter (dotted curve) regimes. The time is normalized with respect to the transit time (t/τ_t).

Figure 8. The diffusion coefficient equivalent in the banana, plateau and PS (solid, dashed and dotted curves, respectively) during the ballistic phase vs time t normalized with respect to the τ_t.

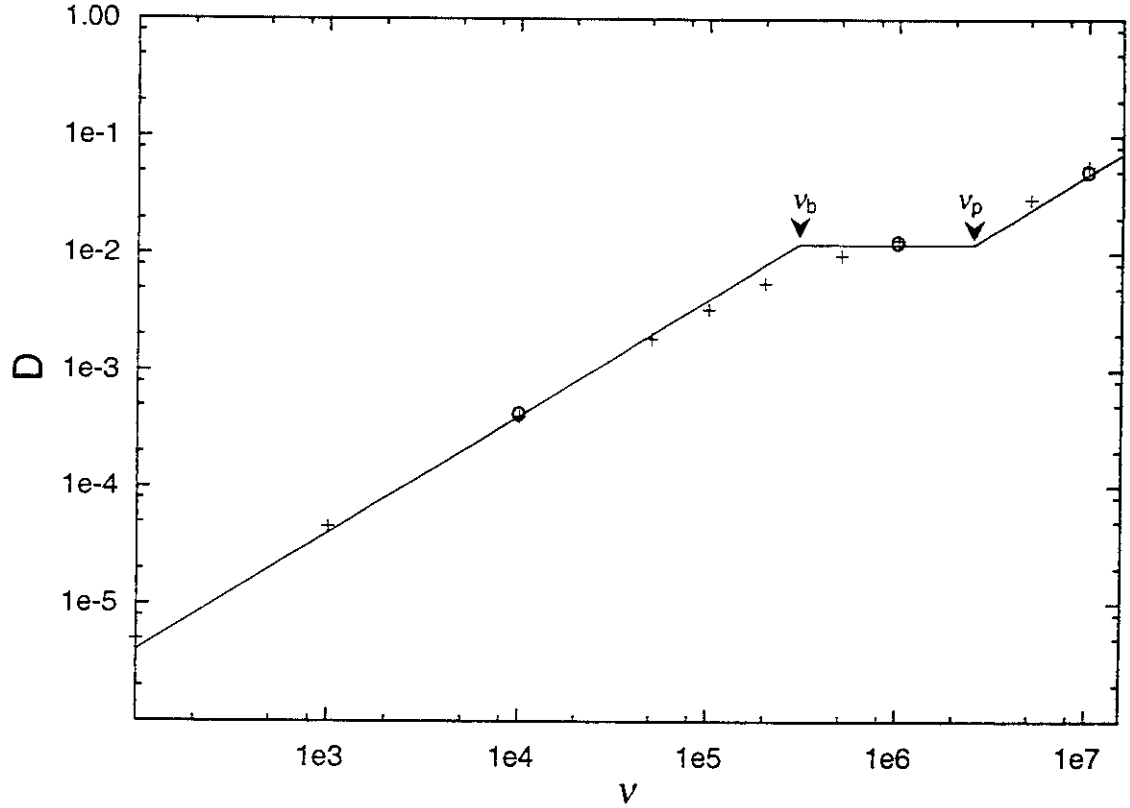
1.00
1e-1
1e-2
1e-3
1e-4
1e-5
D
ν_b
ν_p
1e3
1e4
1e5
1e6
1e7
ν

Fig. 1

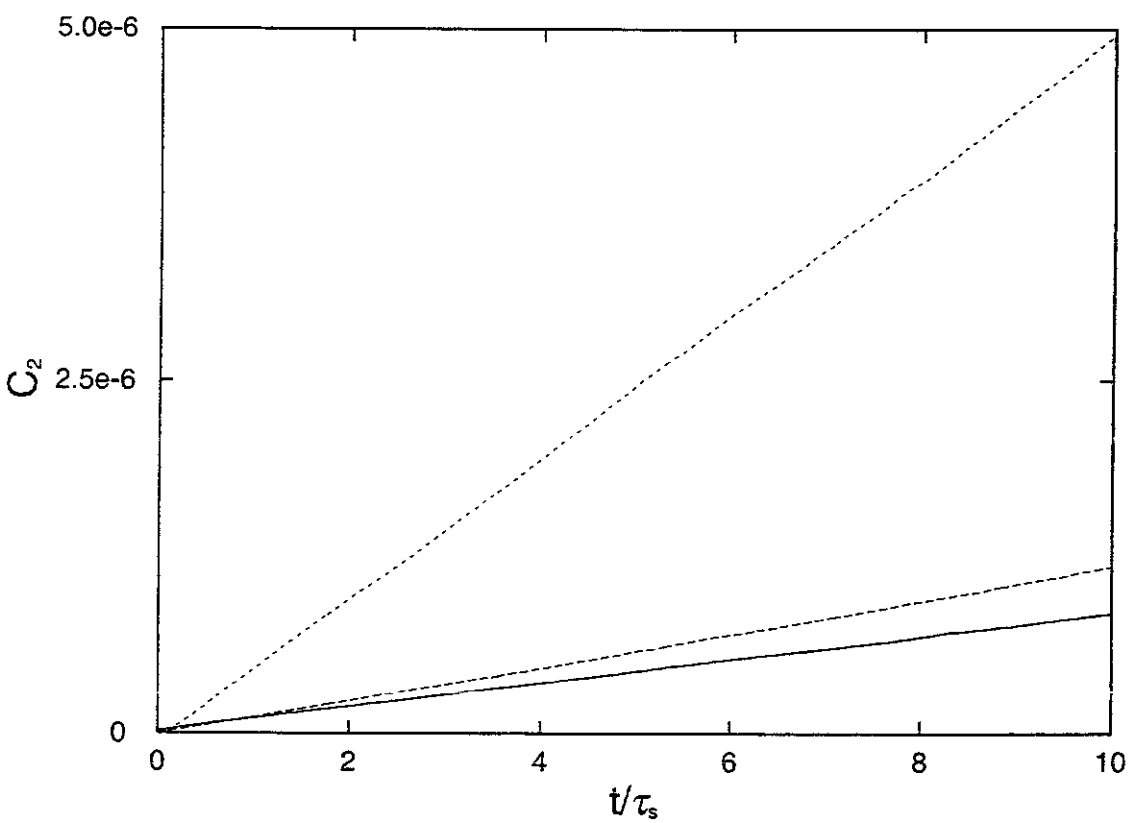
5.0e-6
2.5e-6
0
ζ^2
0
2
4
6
8
10
t/τ_s

Fig. 2

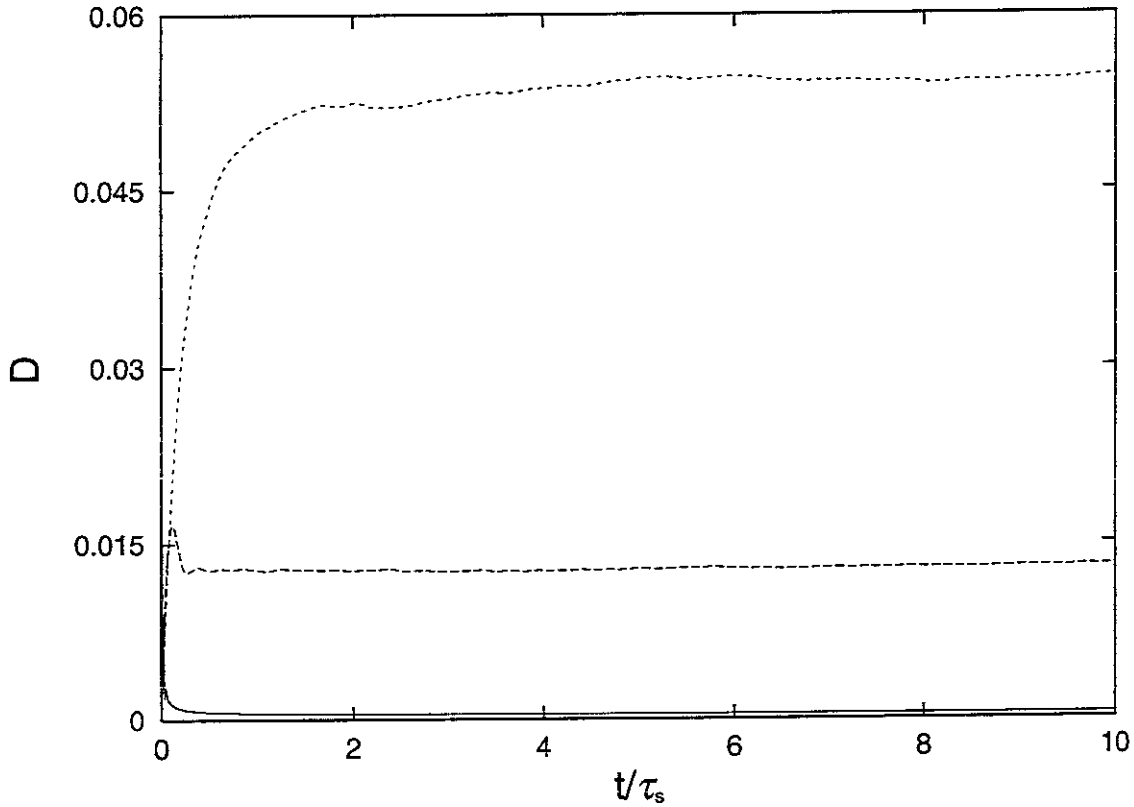

Fig. 3

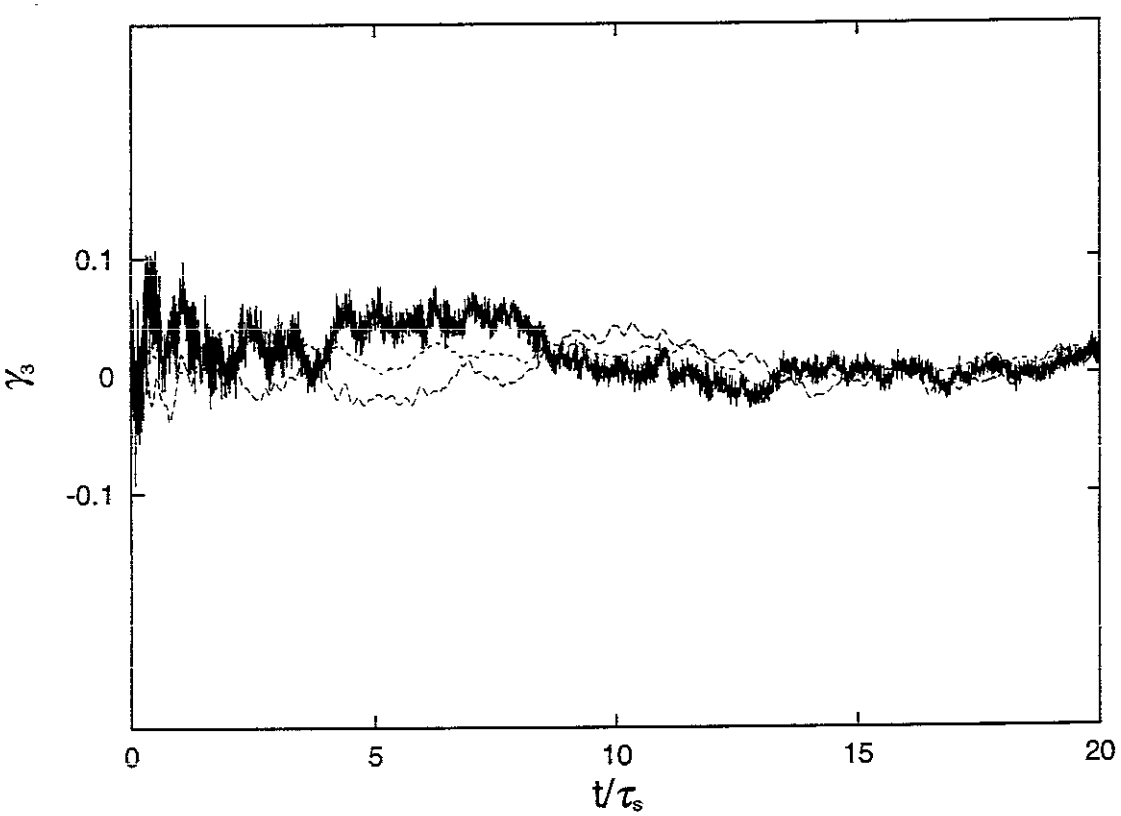

Fig. 4

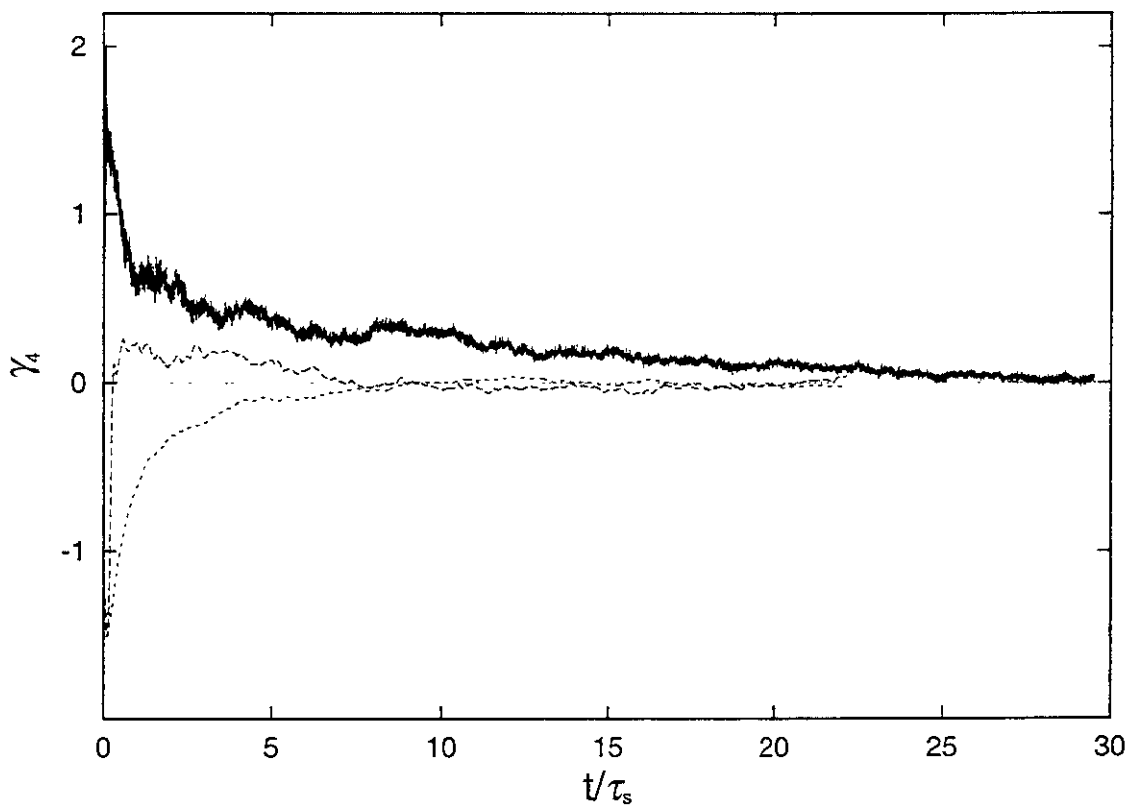
2
1
0
-1
γ_4
0
5
10
15
20
25
30
t/τ_s

Fig. 5

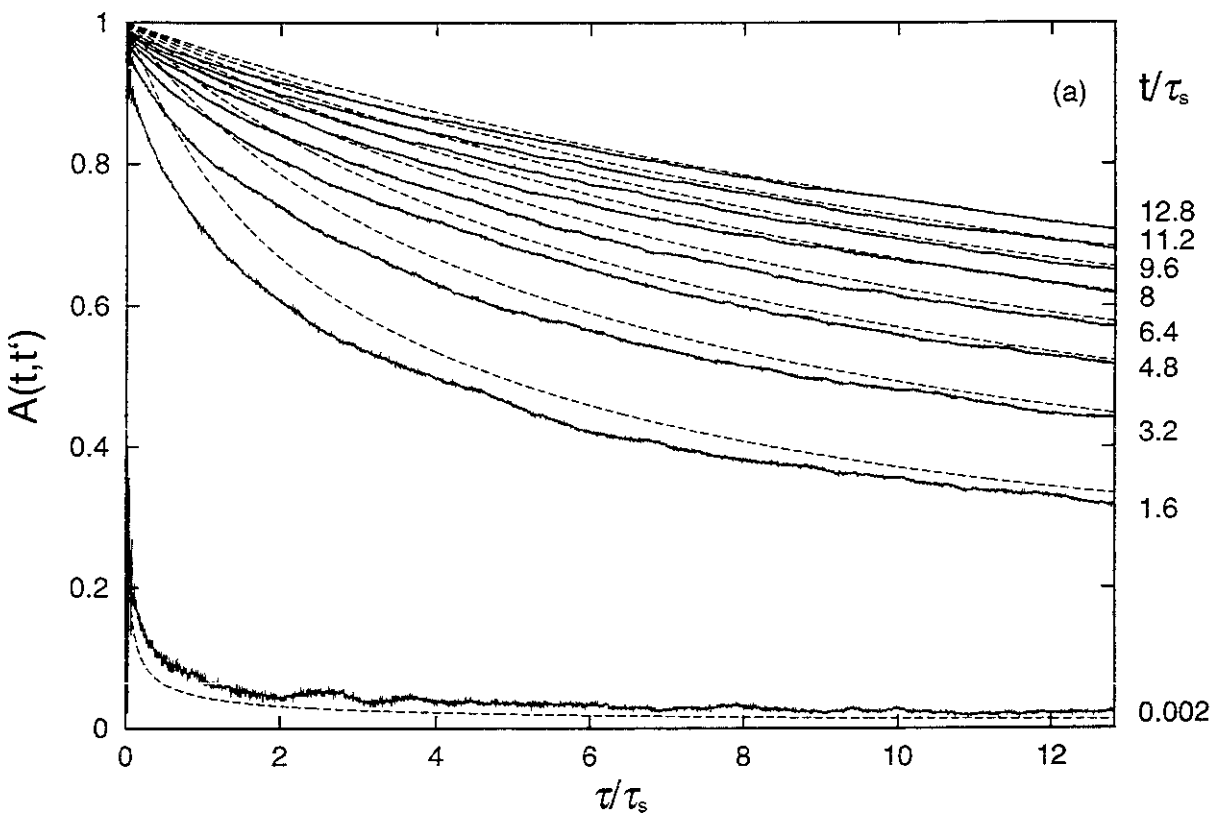
1
0.8
0.6
0.4
0.2
0
A(t,t')
(a)
t/τ_s
12.8
11.2
9.6
8
6.4
4.8
3.2
1.6
0.002
0
2
4
6
8
10
12
τ/τ_s

Fig. 6a

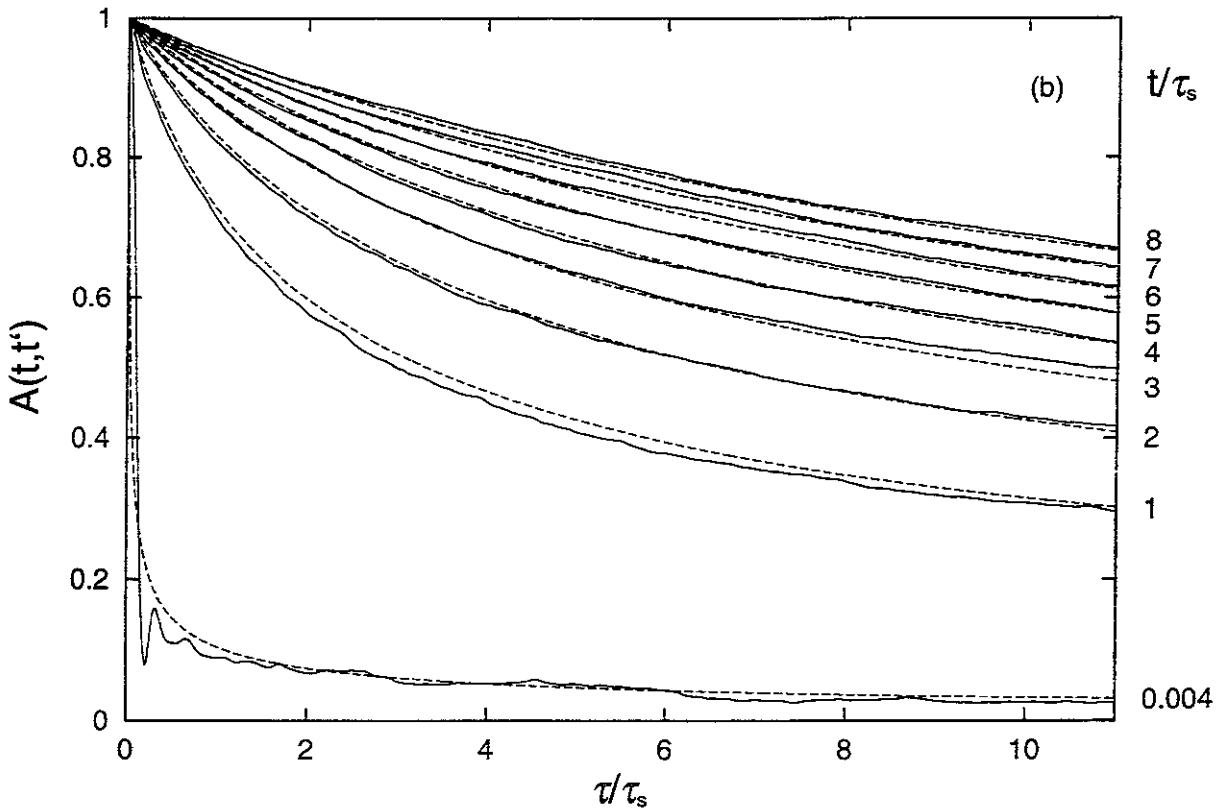
(b)
t/τs
8
7
6
5
4
3
2
1
0.004
A(t,t')
τ/τs
0
0.2
0.4
0.6
0.8
1
0
2
4
6
8
10

Fig. 6b

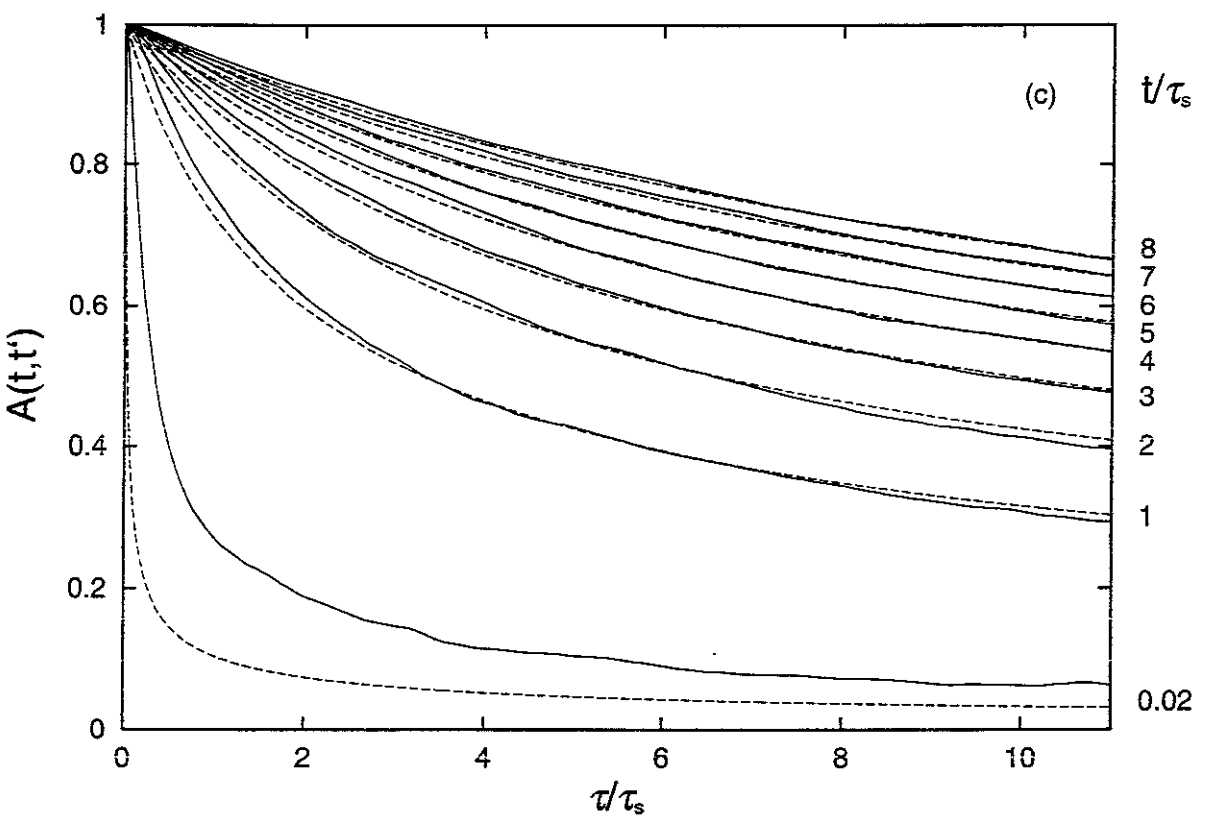
(c)
t/τs
8
7
6
5
4
3
2
1
0.02
A(t,t')
τ/τs
0
0.2
0.4
0.6
0.8
1
0
2
4
6
8
10

Fig. 6c

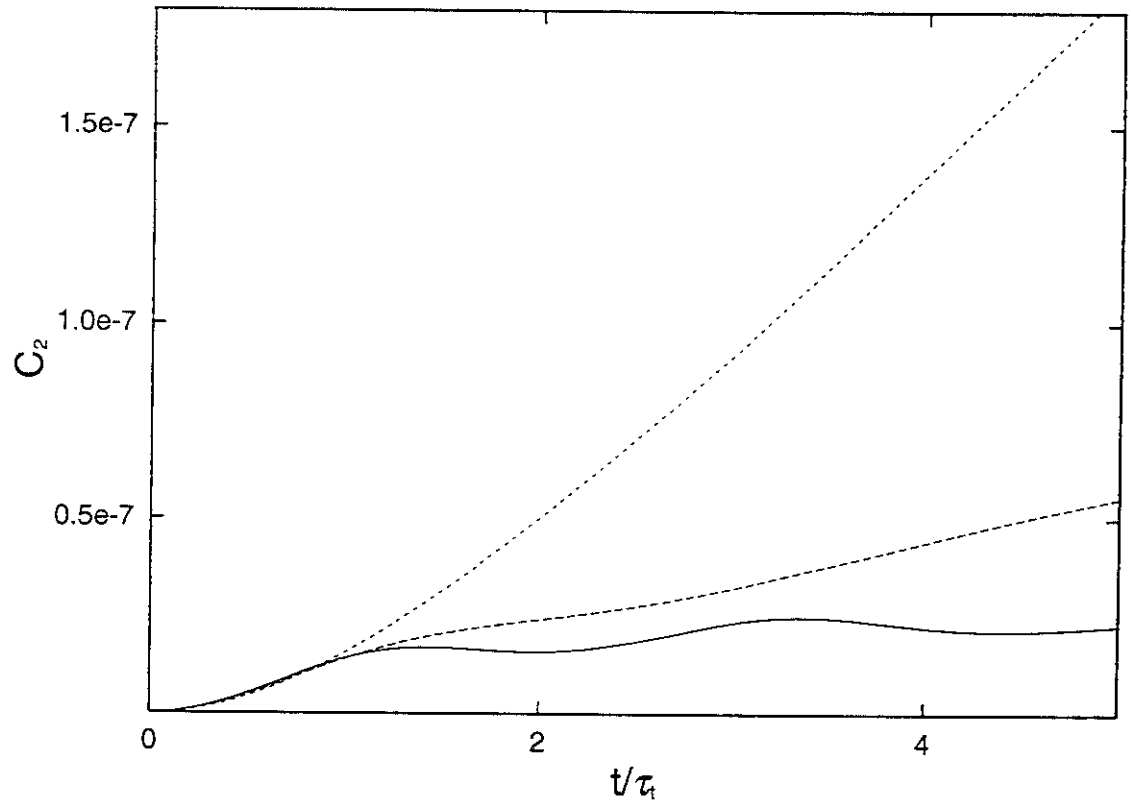

Fig. 7

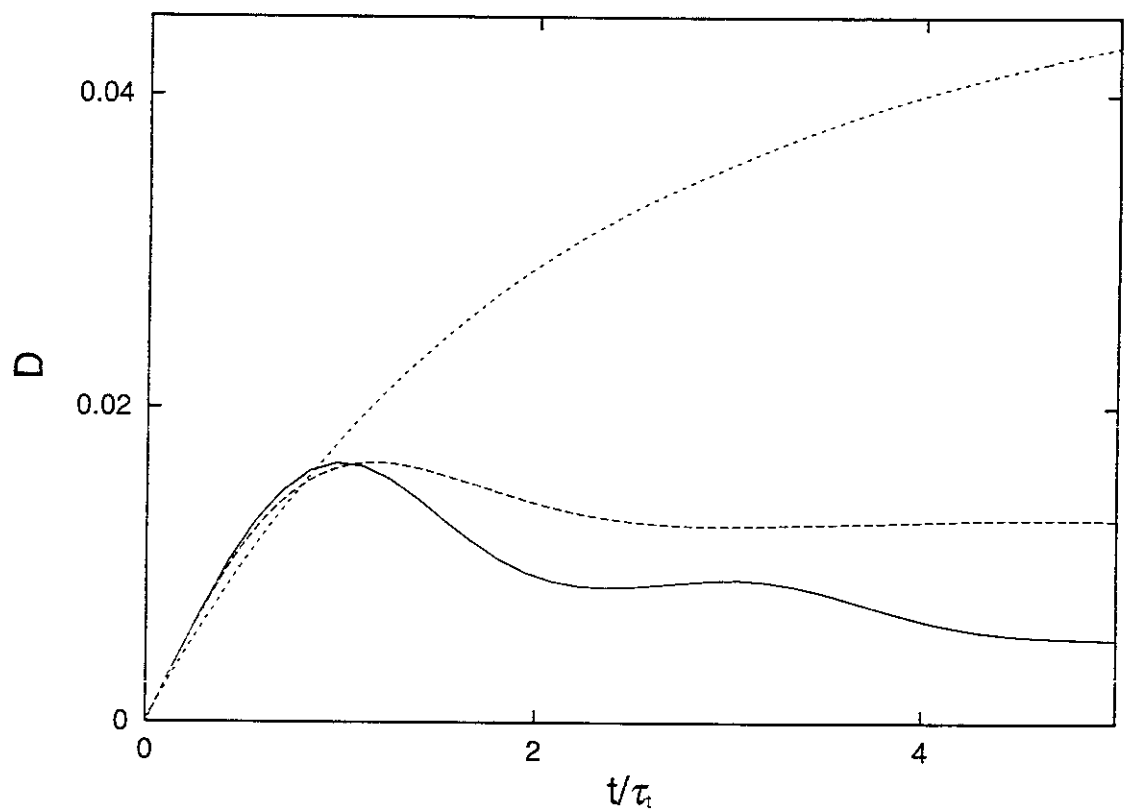

Fig. 8

Recent Issues of NIFS Series

NIFS-665 S Fujiwara and T Sato
Structure Formation of a Single Polymer Chain I Growth of trans Domains Nov 2000

NIFS-666 S Kida
Vortical Structure of Turbulence Nov 2000

NIFS-667 H Nakamura, S Fujiwara and T Sato,
Rigidity of Orientationally Ordered Domains of Short Chain Molecules Nov 2000

NIFS-668 T Mutoh, R Kumazawa, T Seki, K Saito Y Torii F Shimpo, G Nomura T Watari, D A Hartmann, M Yokota, K Akaishi, N Ashikawa, P deVries, M Emoto, H Funaba, M Goto, K Ida, H Idei, K Ikeda, S Inagaki, N Inoue, M Isobe, O Kaneko, K Kawahata, A Komori, T Kobuchi S Kubo, S Masuzaki T Morisaki, S Morita, J Miyazawa, S Murakami, T Minami, S Muto, Y Nagayama, Y Nakamura, H Nakanishi, K Narihara, N Noda K Nishimura, K Ohkubo, N Ohyabu S Ohdachi, Y Oka, M Osakabe, T Ozaki, B J Peterson, A Sagara, N Sato, S Sakakibara, R Sakamoto, H Sasao, M Sasao, M Sato, T Shimozuma, M Shoji, S Sudo, H Suzuki, Y Takeiri, K Tanaka, K Toi, T Tokuzawa, K Tsumori, K Y Watanabe T Watanabe, H Yamada, I Yamada, S Yamaguchi, K Yamazaki, M Yokoyama, Y Yoshimura, Y Hamada, O Motojima, M Fujiwara,
Fast- and Slow-Wave Heating of Ion Cyclotron Range of Frequencies in the Large Helical Device Nov 2000

NIFS-669 K Mima, M S Jovanovic, Y Sentoku, Z-M Sheng M M Skoric and T Sato,
Stimulated Photon Cascade and Condensate in Relativistic Laser-plasma Interaction Nov 2000

NIFS-670 L Hadzievski, M M Skoric and T Sato,
On Origin and Dynamics of the Discrete NLS Equation Nov 2000

NIFS-671 K. Ohkubo, S Kubo, H Idei, T Shimozuma Y Yoshimura, F Leuterer, M Sato and Y Takita,
Analysis of Oversized Sliding Waveguide by Mode Matching and Multi-Mode Network Theory Dec 2000

NIFS-672 C Das, S Kida and S Goto,
Overall Self-Similar Decay of Two-Dimensional Tirbulence Dec 2000

NIFS-673 L A Bureyeva, T Kato, V S Lisitsa and C Namba,
Quasiclassical Representation of Autoionization Decay Rates in Parabolic Coordinates Dec 2000

NIFS-674 L A Bureyeva, V S Lisitsa and C Namba,
Radiative Cascade Due to Dielectronic Recombination Dec 2000

NIFS-675 M FHeyn, S V Kasilof, W Kernbichler, K Matsuoka, V V Nemov, S Okamura, O S Pavlichenko,
Configurational Effects on Low Collision Plasma Confinement in CHS Heliotron/Torsatron, Jan 2001

NIFS-676 K Itoh,
A Prospect at 11th International Toki Conference - Plasma physics, quo vadis?; Jan 2001

NIFS-677 S Satake, H Sugama, M Okamoto and M Wakatani,
Classification of Particle Orbits near the Magnetic Axis in a Tokamak by Using Constants of Motion Jan 2001

NIFS-678 M Tanaka and A Yu Grosberg,
Giant Charge Inversion of a Macroion Due to Multivalent Counterions and Monovalent Coions Molecular Dynamics Studyn, Jan 2001

NIFS-679 K Akaishi, M Nakasuga, H Suzuki, M Iima, N Suzuki, A Komori, O Motojima and Vacuum Engineering Group,
Simulation by a Diffusion Model for the Variation of Hydrogen Pressure with Time between Hydrogen Discharge Shots in LHD, Feb 2001

NIFS-680 A Yoshizawa, N Yokoi, S Nisizima, S -I Itoh and K Itoh
Variational Approach to a Turbulent Swirling Pipe Flow with the Aid of Helicity, Feb 2001

NIFS-681 Alexander A Shishkin
Estafette of Drift Resonances, Stochasticity and Control of Particle Motion in a Toroidal Magnetic Trap Feb 2001

NIFS-682 H Momota and G H Miley,
Virtual Cathode in a Spherical Inertial Electrostatic Confinement Device, Feb 2001

NIFS-683 K Saito R Kumazawa T Mutoh, T Seki, T Watari Y Torii, D A Hartmann Y Zhao A Fukuyama, F Shimpo G Nomura, M Yokota M Sasao, M Isobe, M Osakabe, T Ozaki, K Narihara, Y Nagayama S Inagaki K Itoh, S Morita, A V Krasilnikov K Ohkubo, M Sato S Kubo, T Shimozuma, H Idei Y Yoshimura O Kaneko, Y Takeiri Y Oka K Tsumori, K Ikeda, A Komori H Yamada, H Funaba, K Y Watanabe, S. Sakakibara, M Shoji, R Sakamoto, J Miyazawa, K Tanaka, B J Peterson, N Ashikawa S Murakami T Minami, S Onakachi S Yamamoto, S Kado, H Sasao, H Suzuki, K Kawahata, P deVries, M. Emoto, H Nakanishi, T Kobuchi N Inoue, N Ohyabu, Y Nakamura, S Masuzaki S Muto K Sato, T Morisaki M Yokovama T Watanabe, M Goto, I Yamada, K Ida T Tokuzawa, , N Noda, S Yamaguchi, K Akaishi, A Sagara, K Toi, K Nishimura, K Yamazaki, S Sudo Y Hamada O. Motojima, M Fujiwara,
Ion and Electron Heating in ICRF Heating Experiments on LHD- Mar 2001

NIFS-684 S Kida and S Goto,
Line Statistics Stretching Rate of Passive Lines in Turbulence Mar 2001

NIFS-685 R Tanaka, T. Nakamura and T Yabe.
Exactly Conservative Semi-Lagrangian Scheme (CIP-CSL) in One-Dimension Mar 2001

NIFS-686 S Toda and K Itoh.
Analysis of Structure and Transition of Radial Electric Field in Helical Systems , Mar 2001

NIFS-687 T. Kuroda and H. Sugama,
Effects of Multiple-Helicity Fields on Ion Temperature Gradient Modes Apr 2001

NIFS-688 M. Tanaka,
The Origins of Electrical Resistivity in Magnetic Reconnection: Studies by 2D and 3D Macro Particle Simulations Apr 2001

NIFS-689 A Maluckov N Nakajima, M Okamoto, S Murakami and R Kanno,
Statistical Properties of the Neoclassical Radial Diffusion in a Tokamak Equilibrium Apr 2001